Image Tracking Algorithm using Template Matching and PSNF-*m*

Jong Sue Bae and Taek Lyul Song

Abstract: The template matching method is used as a simple method to track objects or patterns that we want to search for in the input image data from image sensors. It recognizes a segment with the highest correlation as a target. The concept of this method is similar to that of SNF (Strongest Neighbor Filter) that regards the measurement with the highest signal intensity as target-originated among other measurements. The SNF assumes that the strongest neighbor (SN) measurement in the validation gate originates from the target of interest and the SNF utilizes the SN in the update step of a standard Kalman filter (SKF). The SNF is widely used along with the nearest neighbor filter (NNF), due to computational simplicity in spite of its inconsistency of handling the SN as if it is the true target. Probabilistic Strongest Neighbor Filter for m validated measurements (PSNF-*m*) accounts for the probability that the SN in the validation gate originates from the target while the SNF assumes at any time that the SN measurement is target-originated. It is known that the PSNF-*m* is superior to the SNF in performance at a cost of increased computational load. In this paper, we suggest an image tracking algorithm that combines the template matching and the PSNF-*m* to estimate the states of a tracked target. Computer simulation results are included to demonstrate the performance of the proposed algorithm in comparison with other algorithms.

Keywords: Data association, PSNF-*m*, template matching, tracking filter.

1. INTRODUCTION

In case we have prearranged target information, and want to search for and track it, the template matching method is simplest and widely used for detecting targets in image information, which is obtained from IR (infrared) sensor. The Template matching method is searching for the most similar image pattern in the image with a template image obtained from prearranged information. As we use it, it is important what similarity index is used for comparing the template with input image. The similarity index is determined on the following basis [9].

- It does not have to be sensitive to noise of the image.
- It must be insensitive to changing image luminance.
- Its calculation burden must be light.

In many cases, MAD (Mean Absolute Difference), MSE (Mean Square Error), Luminance similarity, Contrast similarity, Correlation, and Hausdorff Distance are used to determine the similarity index by taking the above statements into account [8,17].

In this paper, we choose a correlation as the similarity index and present the scheme in detail, which makes measurements for the tracking filter by using the template matching method in Section 2.

Because a recent target tracking system tends to integrate the signal processing unit for sensor signal and the data processing unit for target tracking, and because it requires real-time signal and data processing, a target tracking algorithm with a lower computational burden and an efficient data association scheme is needed.

In case of single or multi target tracking under a clutter environment, there are Nearest Neighbor algorithm systems (NN), Strongest Neighbor ones (SN), and Probabilistic Data Association ones (PDA) as the data association algorithm that associates the measurements with target tracks. NN uses position information of measurements, SN uses intensity information of measurements, and PDA considers all measurements in the validation gate (VG) [1]. Though PDA algorithm systems have the best performance among these algorithms, they take long time for computation.

Manuscript received July 4, 2007; revised January 7, 2008; accepted February 14, 2008. Recommended by Editorial Board member Jang Myung Lee under the direction of Editor Jae-Bok Song. This research was supported by the Defense Acquisition Program Administration and Agency for Defense Development, Korea, through the Image Information Research Center at Korea Advanced Institute of Science & Technology under the contract UD070007AD.

Jong-Sue Bae is with the Department of Electronic, Electrical, Control and Instrumentation Engineering, Hanyang University, 1271 Sa-1 dong, Sangnok-gu, Ansan, Kyeonggi-do 426-791, Korea (e-mail: bbrother@paran.com).

Taek-Lyul Song is with the School of Electronic and Computer Engineering, Hanyang University, 1271 Sa-1 dong, Sangnok-gu, Ansan, Kyeonggi-do 426-791, Korea (e-mail: tsong@hanyang.ac.kr).

As a component of a system that integrates signal processing with data processing, a tracking filter using a simple, fast, and efficient data association algorithm is a reasonable approach. From this point of view, a tracking filter using an SN data association algorithm is a charming method, and if its track maintenance performance can be made accurate enough, it can be fully applicable.

In this paper, we suggest a target tracking algorithm using a template matching method as well as a PSNF-*m* algorithm to track the target in an image sequence. In Section 3, we explain the PSNF-*m* algorithm, experimental results are given in Section 4, and we conclude the paper in Section 5.

2. TEMPLATE MATCHING FOR MAKING MEASUREMENT

2.1. Template matching by using correlation

Refer to introduction: various similarity indices are used in the template matching method. In this paper, we make use of statistical correlation between the template and overlapped area in the input frame as similarity index defined as (1).

$$S(T,I) = \frac{\sigma_{TI} + C_2}{\sigma_T \sigma_T + C_2}, \tag{1}$$

where

$$\sigma_{TI} = \frac{1}{MN-1} \sum_{i=0}^{M} \sum_{j=0}^{N} \{T(X_i, Y_j) - \mu_T\}\{I(X_i, Y_j) - \mu_I\}. \tag{2}$$

μ_T and σ_T correspond to the mean and standard deviation of template intensity respectively. μ_I and σ_I correspond to the mean and standard deviation of intensity of overlapped area in the input frame respectively. The constant C_2 is included to avoid instability when the denominator is very close to zero. Because $S(T,I)$ is a correlation value, its range is $-1 \le S(T,I) \le 1$. As the $S(T,I)$ value gets closer to 1, the overlapped area in the input frame is very similar to the template. Therefore we regard the position with the maximum value of $S(T,I)$ as the target position.

2.2. Signal intensity distribution of target and clutter

The target tracking filter, such as PSNF-*m* which we will explain in Section 3, uses a point measurement of target and clutter. But the template matching result is not a point but an area. Therefore, it is necessary to define the target and clutter to get the measurement used in the PSNF-*m* algorithm.

Target measurement position is defined as the center position of the area of which correlation, greater than the threshold, is the greatest one among the other ones over the threshold as the result of template matching. Target intensity is defined as the correlation value. Like the preceding, clutter position is defined as the center position of the area of which correlation is greater than the threshold except that of the target. Clutter intensity is defined as its correlation value.

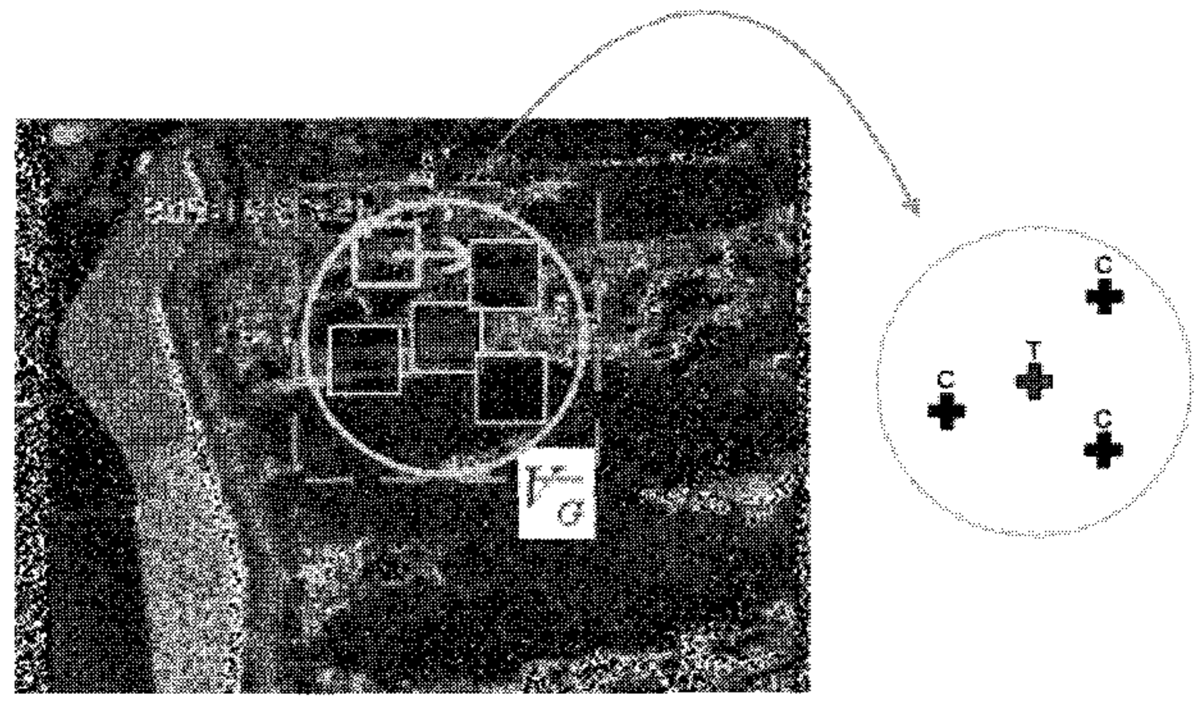

Fig. 1. Definition of target and clutter.

While deriving the PSNF-*m* algorithm, we assume that target and clutter signal intensity have the Gaussian distribution. Distribution parameters, such a mean and standard deviation, are obtained from experimental images and they apply to the PSNF-*m* algorithm.

At first, we create a noisy environment by adding Gaussian noise to find the parameters of the intensity distribution. Regarding the designated position as target, we perform the template matching to the entire image. In this way, we can classify the target and clutter signal because we know where the target is and where the clutters are.

When we accomplish the template matching with the 24×24 size template for the 320×240 size search image, approximately 64000 measurements are generated per one frame. The distribution of the clutter signal is obtained by drawing a histogram of measurements, except a target measurement from all

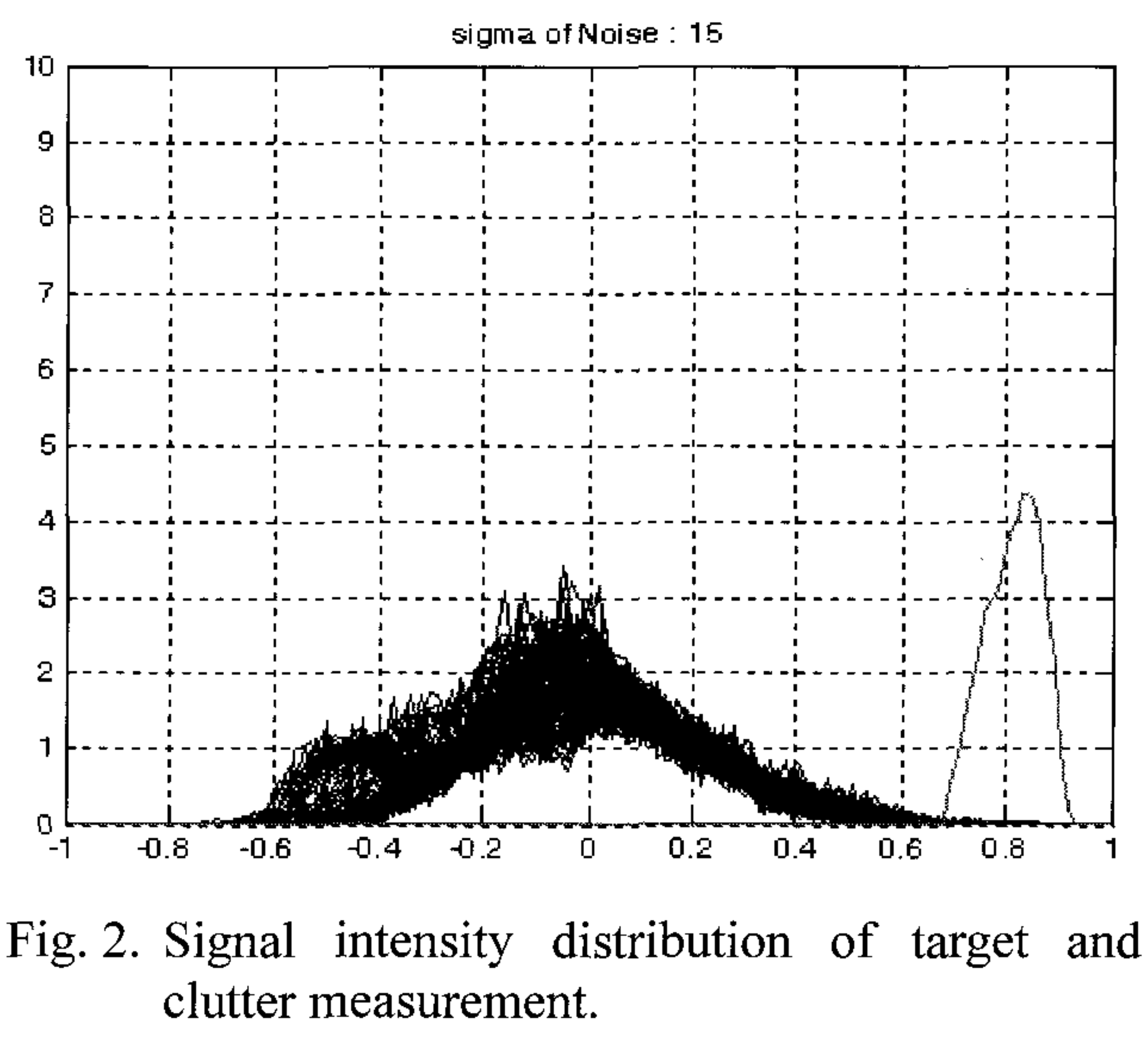

Fig. 2. Signal intensity distribution of target and clutter measurement.

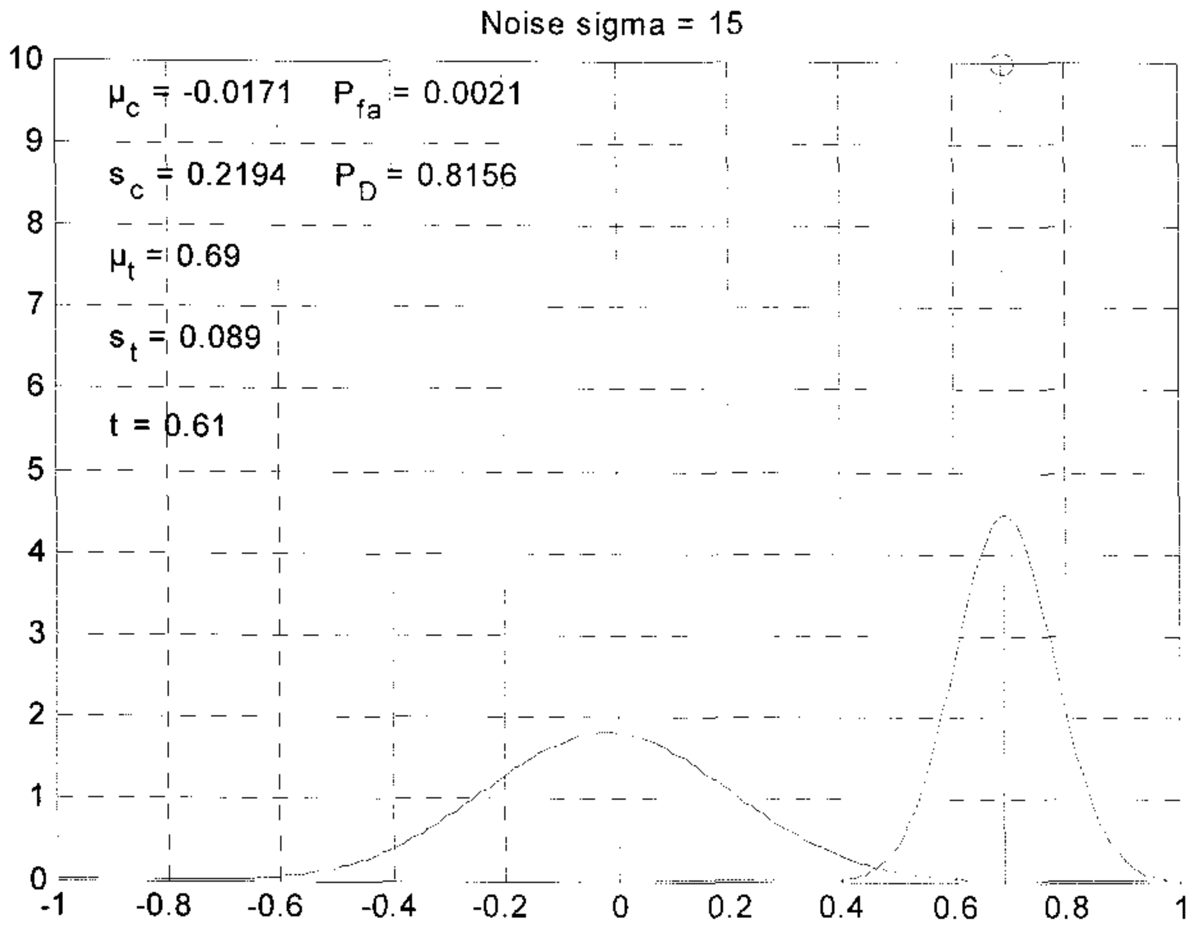

Fig. 3. Approximated Gaussian distribution of target and clutter intensity.

measurements. Since clutter measurements are taken as large numbers from just one frame, about 10 frames are enough to obtain the clutter distribution.

Because we can get just one target measurement per frame, we must perform template matching for many more frames to calculate target intensity distribution. Therefore we do this for about 300~400 frames to gather target measurement information.

Fig. 2. shows the histogram of target and clutter signal intensity after Gaussian noise of which standard deviation of 15 is added to the search image.

On the basis of information gotten from Fig. 2, we can approximate the distribution of target and clutter to the Gaussian distribution represented in Fig. 3.

2.3. CA-CFAR algorithm to arrange the measurements

When using the template matching method to generate the measurements, matching is performed moving the mask pixel by pixel in the VG, and it makes too many measurements per frame.

The PSNF-*m* algorithm presented in this paper sorts the measurements by intensity and chooses the maximum intensity measurement for the filter update step. If there are excessive measurements in the VG, it takes much time to sort the measurements. And because the PSNF-*m* algorithm is limited in that the maximum measurement number is m, the number of measurements in the VG must be restricted to m or less.

To solve this problem, an algorithm that doesn't get rid of the target measurement but reduces the number of clutter measurements efficiently is needed.

Constant false alarm rate (CFAR) processors are useful for detecting targets in background for which all parameters in the statistical distribution are not known and may be nonstationary [13]. The threshold in a CFAR detector is set on a cell by cell basis using estimated noise power by processing a group of reference cells surrounding the cell under investigation [13].

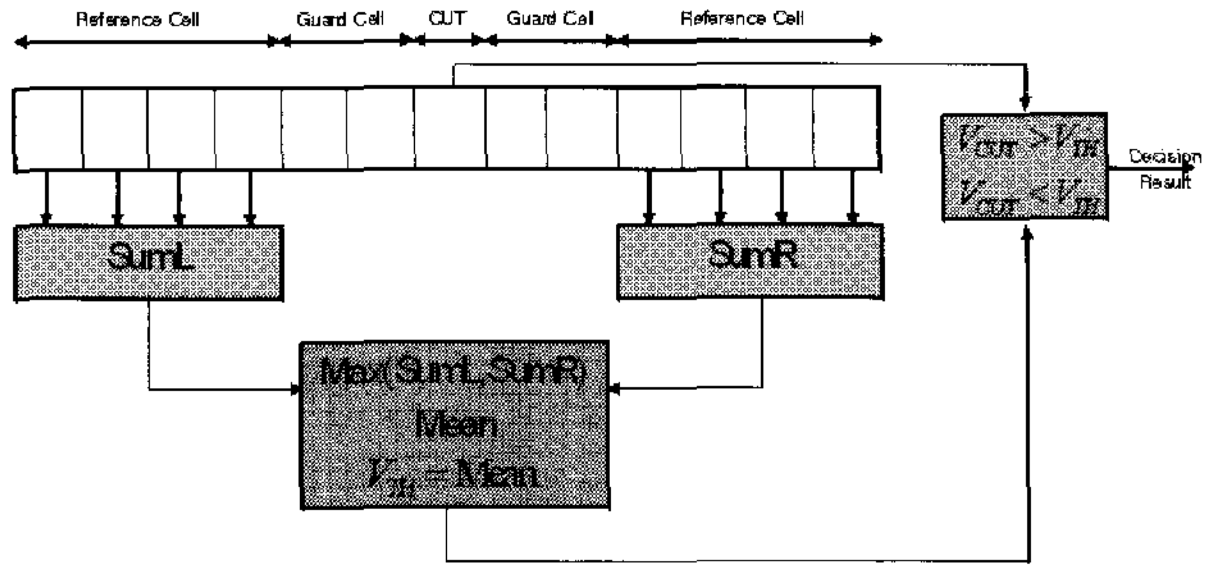

Fig. 4. GOCA-CFAR method.

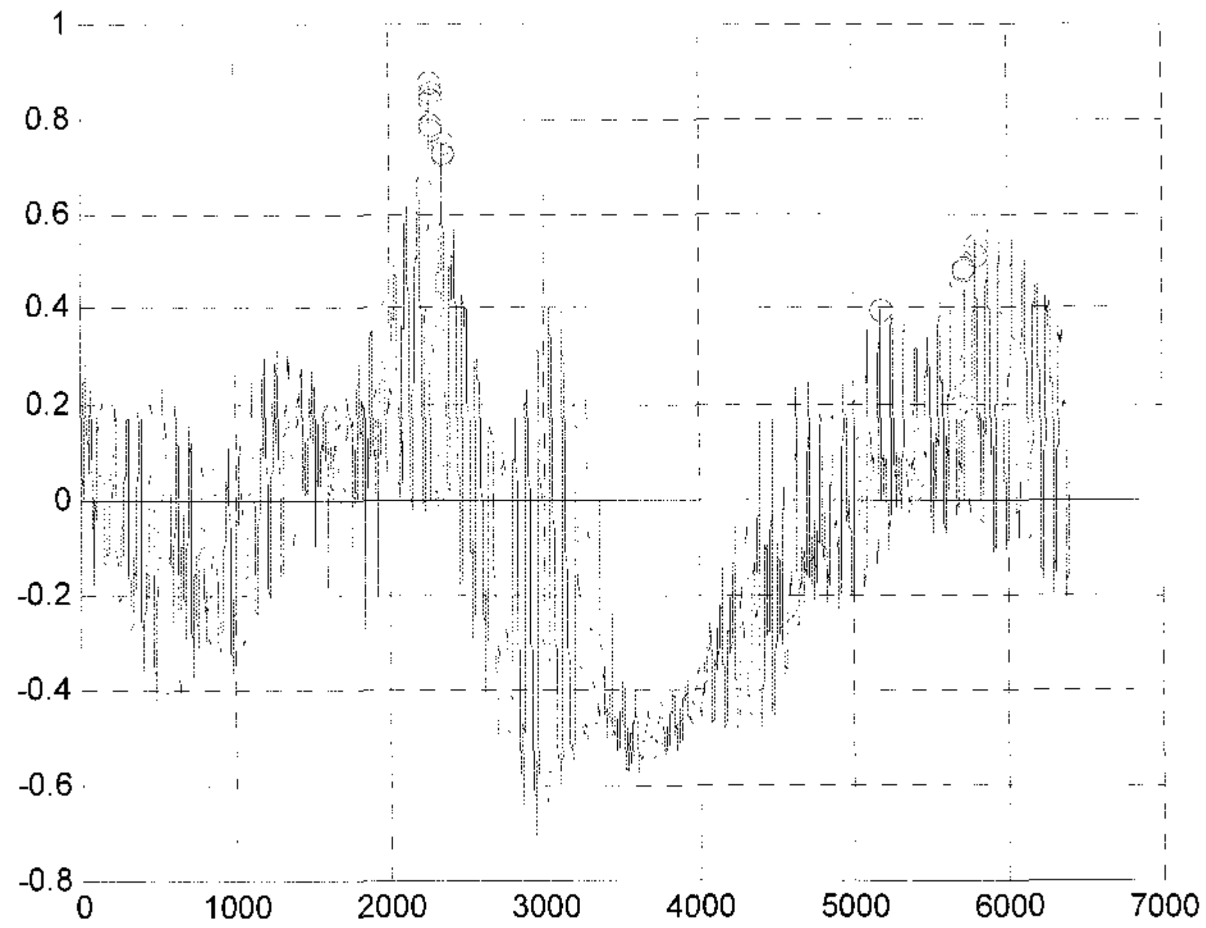

Fig. 5. Result of GOCA-CFAR.

The widely used CFAR algorithms are "Cell Averaging (CA)-CFAR," "Greatest Of' (GO)-CFAR," "Smallest Of' (SO)-CFAR," "Order Statistics (OS)-CFAR," and "Trimmed Mean (TM)-CFAR" [12-15].

Among the abovementioned CFAR algorithms, we apply Greatest Of Constant Average (GOCA) CFAR to the template matching method to reduce the measurements until its number is under m. Fig. 4 is the block diagram of the GOCA-CFAR algorithm.

Fig. 5 shows the result of adapting this algorithm to the measurement to arrange it. The result in Fig. 5 is obtained by running the GOCA-CFAR algorithm beginning with 6400 measurements until its number is 13 or less.

3. TARGET TRACKING BY USING PSNF-M ALGORITHM

3.1. PSNF-*m* algorithm

The existing probabilistic strongest neighbor filter (PSNF) accounts for the probability that the strongest neighbor (SN) in the validation gate is originated from the target while the strongest neighbor filter (SNF) assumes at any time that the SN measurement is target-originated. The PSNF-*m* algorithm is a modified form of the probabilistic strongest neighbor filter (PSNF) algorithm [3] taking into account the number of validated measurements [2,7]. It is known that the existing PSNF-*m* is superior to the SNF and PSNF in tracking performance. The PSNF-*m* algorithm is developed to reduce the computational load, which is the defect of the PSNF algorithm, and to adapt it for a real environment of which exact clutter density cannot be gotten by calculating target probability density, as PDAF-AI [4], correlated with 3 events, which selects the SN measurement by considering the number of measurements in the validation gate whose center is the current target's predicted position [2]. The problem of SNF is solved by applying the Bayesian approach. Viewing from the Bayesian standpoint, target tracking is to update the conditional probability density function (cpdf) recursively, which means the current target's status when the cumulating sensor measurements and the priori information are given. Therefore it is very important for solving the problem of SNF to calculate the cpdf of the target state variable in case of being given the possible event correlated with the data association that uses the SN measurement. As a result of applying the Bayesian approach to calculate the cpdf of the SN measurement, the PSNF, in contrast to the PDAF, accounts for the probability of the possible events that is correlated with the data association method using the SN measurement. The PSNF-*m* algorithm is to improve the PSNF algorithm by regarding the cpdf of the SN measurement as the function of the *m* validated measurements in the validation gate.

In contrast to the PSNF-*m* proposed in [2], we suppose that the target and clutter signal intensity are based on the Gaussian distribution, and the new algorithm is proposed in this paper. The following 8 assumptions are used in this paper.

Assumption 1: The measurement signal intensity 'a' is Gaussian-distributed with probability density function (pdf)

$$f_1(a)=\frac{1}{\sqrt{2\pi}\sigma_t}\exp\left(-\frac{(a-v_t)^2}{2\sigma_t^2}\right). \tag{3}$$

The clutter signal amplitude satisfies

$$f_0(a)=\frac{1}{\sqrt{2\pi}\sigma_c}\exp\left(-\frac{(a-v_c)^2}{2\sigma_c^2}\right). \tag{4}$$

Assumption 2: The number of validated true measurement is denoted by m^T, and m^T is at most 1. The probability that $m^T=1$ is $P(m^T=1)=P_DP_G$ where P_D is the probability of target detection indicating that the target signal amplitude exceeds a threshold τ; and P_G is the probability that the target falls inside the validation gate. P_D satisfies

$$P_D=\int_\tau^\infty f_1(a)da \tag{5}$$

from Assumption 1, and the probability that the false measurement signal exceeds the threshold τ is

$$P_{fa}=\int_{-\infty}^\tau f_0(a)da. \tag{6}$$

Assumption 3: The number of validated false measurements in the validation gate, denoted by m^F, is Poisson distributed with a spatial density λ such that

$$\mu_F(m)=P(m^F=m)=\frac{(\lambda V_G)^m}{m!}e^{-\lambda V_G}.$$

The volume of the n-dimensional gate satisfies $V_G=C_n|S|^{\frac{1}{2}}\gamma^{\frac{n}{2}}$ where $|S|$ is the determinant of covariance of residual, $\sqrt{\gamma}$ is gate size and $C_1=2$, $C_2=\pi$, $C_3=\frac{4}{3}\pi$ etc.

Assumption 4: The state prediction error $\bar{e}_k=x_k-\bar{x}_k$ for any given time k is a zero-mean Gaussian process with a covariance $\bar{P}_k$ such that

$$\bar{e}_k\sim N(\bar{e}_k;0,\bar{P}_k). \tag{7}$$

Assumption 5: The validated false measurements at any time are i.i.d. uniformly distributed over the gate.

Assumption 6: The location and amplitude of a validated false measurement are independent of the true measurement at any time and other validated false measurements at any other time.

Assumption 7: Amplitude is independent of the location.

Assumption 8: The target is existing and can be detectable, i.e., it is perceivable [6].

There exist the following three events related to data association with the SN measurement.

M_T: The SN measurement is target-originated.

M_F: The SN measurement is from a false target.

M_0: There is no validated measurement.

Because the derivation of PSNF-*m* with the eight assumptions above and possible three events to select the SN measurement is fully presented in [7], it is omitted in this paper. The SN data association algorithm, which uses signal amplitude to identify the target uses it to do the target: however, it uses position information of SN to update the filter states. From the Assumption 7, this amplitude information and position information is independent of each other. The PSNF algorithm uses signal amplitude information for calculating the probability of M_T and M_F. We use the pdf of signal amplitude of M_T and M_F obtained in Section 2.2.

Under the conditions that the number of validated measurements is m and the SN measurement is target-originated, the cpdf of the signal amplitude $a^T = a$ satisfies the following Bayes' rule [5]

$$f\left(a \middle| M_T, m\right) = \frac{1}{P\left(M_T, m\right)} f\left(a, M_T, m\right), \tag{8}$$

where $f\left(a, M_T, m\right)$ is the joint pdf in which the validated target amplitude $a^T = a$ is the strongest among the m validated measurements under the assumptions of $m^T = 1$ and $m^F = m-1$. Applying the Bayes' rule [5] again to $f\left(a, M_T, m\right)$ satisfies

$$\begin{aligned} &f\left(a, M_T, m\right) \\ &= P\left(M_T \middle| a^T = a, m^T = 1, m^F = m-1\right) \\ &\quad \cdot f\left(a \middle| m^T = 1, m^F = m-1\right) \\ &\quad \cdot P\left(m^T = 1\right) P\left(m^F = m-1\right). \end{aligned} \tag{9}$$

Similarly, under the conditions that the number of validated measurements is m and the SN measurement is clutter-originated, the cpdf of the signal amplitude $a^F = a$ satisfies the following Bayes' rule

$$f\left(a \middle| M_F, m\right) = \frac{1}{P\left(M_F, m\right)} f\left(a, M_F, m\right), \tag{10}$$

where $f\left(a, M_F, m\right)$ is the joint pdf in which the validated target amplitude $a^F = a$ is the strongest among the m validated measurements under the assumption that the number of validated false measurements m^F is over 1 and the number of target m^T can be 0 or 1. Applying the Bayes' rule to $f\left(a, M_F, m\right)$ satisfies

$$\begin{aligned} &f\left(a, M_F, m\right) \\ &= P\left(M_F \middle| a^F = a, m^T = 0, m^F = m\right) \\ &\qquad f_{C_1}\left(a \middle| m^F = m\right) \times P\left(m^T = 0\right) \mu_F(m) \\ &\quad + P\left(M_F \middle| a^F = a, m^T = 1, m^F = m-1\right) \\ &\qquad f_{C_1}\left(a \middle| m^F = m-1\right) \times P\left(m^T = 1\right) \mu_F(m-1). \end{aligned} \tag{11}$$

$f_{C_1}\left(a \middle| m^F = m\right)$ denotes the cpdf of amplitude a of the clutter-originated SN measurement, of which amplitude higher than the threshold τ, under the assumption that the number of validated false measurements $m^F = m$ and $f_{C_1}\left(a \middle| m^F = m-1\right)$ denotes the cpdf of amplitude a of the clutter-originated SN measurement under the assumption $m^F = m-1$ [7]. In the case of $\bar{M}_0$, it is necessary to know the number of measurements m and the distribution $f(D^T | M_F, m)$ to derive the covariance update algorithm. D^T is the normalized distance squared (NDS) of the target. Note that the NDS of a measurement z_k is defined as $D_k = (z_k - \bar{z}_k)^T S_k^{-1}(z_k - \bar{z}_k)$ in which $\bar{z}_k$ is the predicted measurement and S_k is the measurement residual covariance matrix. If we represent $D^T = D$, $f(D^T | M_F, m)$ is expressed as

$$\begin{aligned} &f(D^T | M_F, m) \\ &= \frac{1}{P(M_F, m)} f(D^T, M_F, m) \\ &= \frac{nV_{D^T}}{2D^T} N(D^T) \\ &\frac{(1 - P_D \cdot 1(\gamma - D^T))\mu_F(m) + P_D(1 - \bar{P}_A) \cdot 1(\gamma - D^T)\mu_F(m-1)}{(1 - P_D P_G)\mu_F(m) + P_D P_G(1 - \bar{P}_A)\mu_F(m-1)}. \end{aligned} \tag{12}$$

The probability weighting for $\bar{M}_0$ is evaluated from the a posteriori probabilities as

$$\beta_1 = \frac{f\left(D, a, M_T, m\right)}{f\left(D, a, M_T, m\right) + f\left(D, a, M_F, m\right)}, \tag{13}$$

where by Assumptions 5 and 7

$$\begin{aligned} f(D, a, M_T, m) &= f(D | a, M_T, m) f(a, M_T, m) \\ &= f(D | M_T) f(a, M_T, m), \end{aligned} \tag{14}$$

$$f(D, a, M_F, m) = f(D | M_F) f(a, M_F, m). \tag{15}$$

Note that $f(D | M_T) = \frac{N(D)}{P_G}$, $f(D | M_F) = \frac{1}{V_G}$, and $f(a, M_T, m)$ and $f(a, M_F, m)$ are expressed in (9) and (11) respectively. The PSNF-*m* algorithm is summarized in Table 1.

In Table 1, the constant $0 \le C_{Tg} \le 1$ is a scaling factor for the gating effect on the residual covariance [3] and it satisfies

$$C_{Tg} = \frac{1}{P_G} \int_{V_G} N(v^t; 0, S) dv^t = \frac{\int_0^\gamma q^{\frac{n}{2}} e^{-\frac{q}{2}} dq}{n \int_0^\gamma q^{\frac{n}{2}-1} e^{-\frac{q}{2}} dq}, \tag{28}$$

K is the Kalman gain, and S stands for the measurement residual covariance.

Table 1. PSNF-m algorithm.

(1) Prediction step

Identical to the standard Kalman filter

(2) Update step

① For the case of M_0

$$\hat{x}_k = \bar{x}_k \tag{16}$$

$$\hat{P}_k = \bar{P}_{k,M0} = \bar{P}_k + \frac{P_D P_G (1 - C_{Tg})}{1 - P_D P_G} KSK^T \tag{17}$$

② For the case of $\bar{M}_0$

$$\bar{P}_A = 1 \quad for \quad m = 1 \tag{18}$$

$$\hat{x}_k = \bar{x}_k + K\beta_1 v^*, \quad v^* = z_k - H\bar{x}_k \tag{19}$$

$$\hat{P}_k = \bar{P}_{k,M_F}(1 - \beta_1) + (\bar{P}_k - KSK^T)\beta_1 + \beta_0 \beta_1 K v^* v^{*T} K^T \tag{20}$$

where

$$\bar{P}_{k,M_F} = \bar{P}_k - KSK^T + \frac{(1 - P_D P_G C_{Tg})\lambda V_G + P_D P_G C_{Tg}(1 - \bar{P}_A)m}{(1 - P_D P_G)\lambda V_G + P_D P_G (1 - \bar{P}_A)m} KSK^T \tag{21}$$

$$\bar{P}_A = \frac{1}{P_D} \int_\tau^\infty N_1(a) \left[1 - \frac{1}{P_{fa}} \int_\tau^\infty N_0(a') da' \right]^{m-1} da \tag{22}$$

$$(\bar{P}_A = 1 \text{ for } m = 1) \tag{23}$$

$$\beta_1 = \frac{f(D, a, M_T, m)}{f(D, a, M_T, m) + f(D, a, M_F, m)} = \frac{\beta_{1A}}{\beta_{1A} + \beta_{1B} + \beta_{1C}} \tag{24}$$

where

$$\beta_{1A} = T_c N_1(a) N_1(D)$$

$$\beta_{1B} = (1 - P_D P_G)\lambda T_c \frac{N_1(a)}{P_{fa}}$$

$$\beta_{1C} = P_G [P_D + G_t - 1](m-1) \frac{N_0(a)}{P_{fa}} \frac{1}{V_G}$$

$$T_c = 1 + \frac{G_c - 1}{P_{fa}} \tag{25}$$

$$G_c = G\left(\frac{a - \mu_c}{\sigma_c}\right) = \int_{-\infty}^a N_0(a') da'$$

$$G_t = G\left(\frac{a - \mu_t}{\sigma_t}\right) = \int_{-\infty}^a N_1(a') da'$$

$$N_0(a) = \frac{1}{\sqrt{2\pi}\sigma_c} \exp\left(-\frac{(a - \mu_c)^2}{2\sigma_c^2} \right) \tag{26}$$

$$N_1(a) = \frac{1}{\sqrt{2\pi}\sigma_t} \exp\left(-\frac{(a - \mu_t)^2}{2\sigma_t^2} \right)$$

$$N_1(D) = \frac{1}{2\pi |s|^{1/2}} \exp\left(-\frac{D}{2} \right)$$

$$\beta_0 = 1 - \beta_1 \tag{27}$$

3.2. Track initiation with track score

Track score μ_k is calculated to initiate the PSNF-m filter and to decide whether to maintain the track or not. Assuming that the target and clutter signal amplitude follow the Gaussian distribution, μ_k can be described by

$$\mu_k = \frac{(1 - \delta)\bar{\mu}_k}{1 - \delta \bar{\mu}_k}, \tag{29}$$

where

$$\bar{\mu}_k = \Pi_{11}\mu_{k-1} + \Pi_{10}(1 - \mu_{k-1}), \tag{30}$$

$$\delta = P_D P_G - \frac{m}{\lambda V_G} P_D P_G (1 - \bar{P}_A(m)) - \frac{m}{\lambda} P_D N_1(z_k) \bar{P}_A(m), \tag{31}$$

and $\bar{P}_A(m)$ is given by (22).

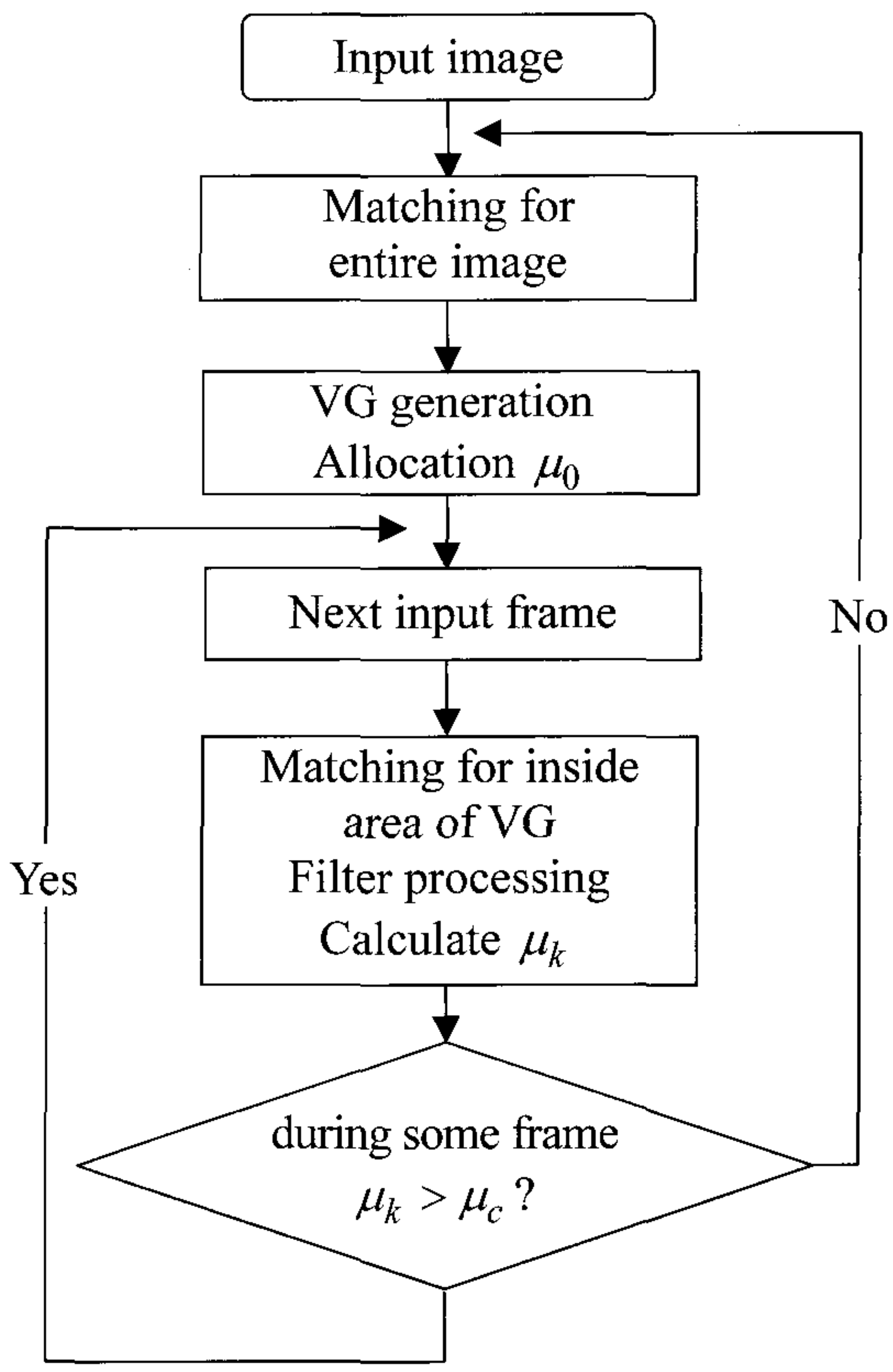

Fig. 6. Target tracking filter flow chart.

To initiate the filter, the following steps are processed.

a) We perform the template matching to the whole search image by using the given template. As the result of matching, we allocate the VG whose center is equal to the area's center that has the largest correlation value. We also initiate the track score as μ_0.

b) When the next frame is given, we perform the matching only to the inside of VG and select the SN measurement. Then we can initiate the filter state variables and parameters by using two measurements from the first and second frame and calculate the track score μ_k.

c) We compute the track score μ_k for every sequential input frame. If μ_k remains smaller than μ_c before the fixed frame, its track is terminated and a new target track is generated.

Fig. 6 is the flow chart of the tracking filter.

4. SIMULATION RESULTS

Target tracking simulation is accomplished by the input movie with AVI format. The rate of the input movie is 33 frames/sec and the PSNF-*m* filter is processed for each frame.

The simulation program is roughly organized into three parts, which are template matching, GOCA-CFAR, and PSNF-*m* filter.

We use a 24×24 size template such as Fig. 8 from the reference image to process the template matching

After the template is generated, we add the Gaussian noise to the input frame to make a noisy environment. The mean of Gaussian noise is 0 and the standard deviation is 15.

Template matching is executed for the entire noise-added image when the tracking filter is not initiated yet. In contrast to the above statement, when the filter is initiated, matching is performed to the inside of VG to get the measurements. If the filter track isn't initiated, it has to be initiated at first. The track initiation is processed by applying the method proposed in Section 3.2. After track initiation, we perform the filter update and prediction step and calculate the track score to determine whether to maintain the track or not for every frame.

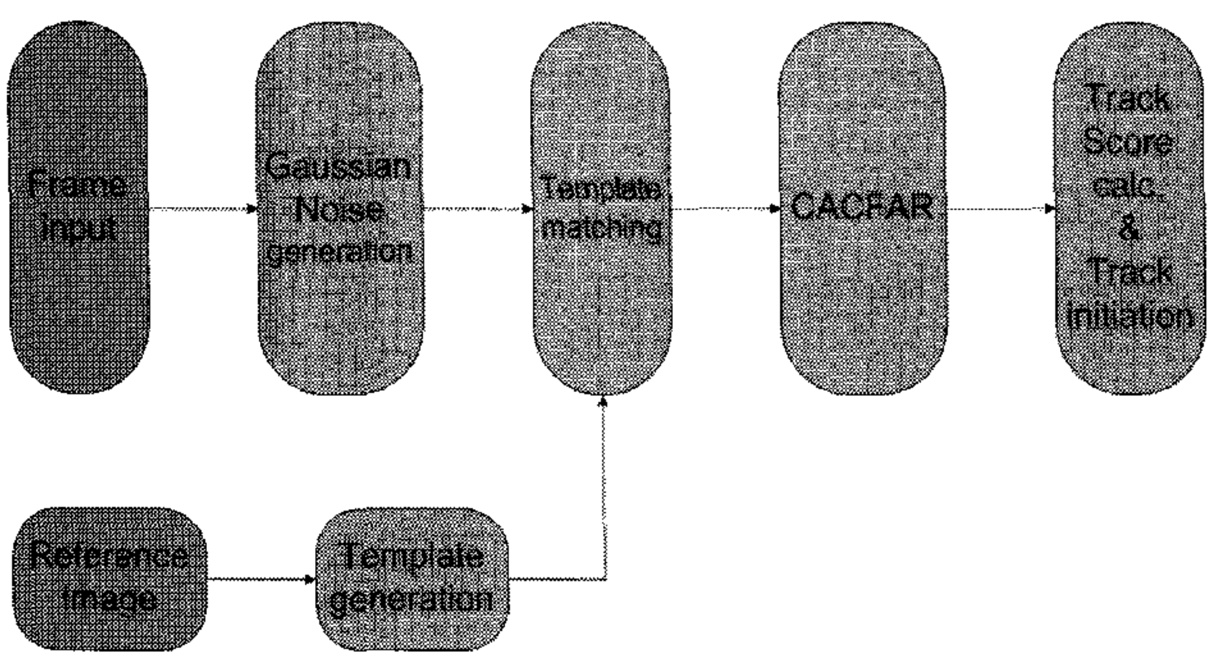

Fig. 7. Simulation block diagram.

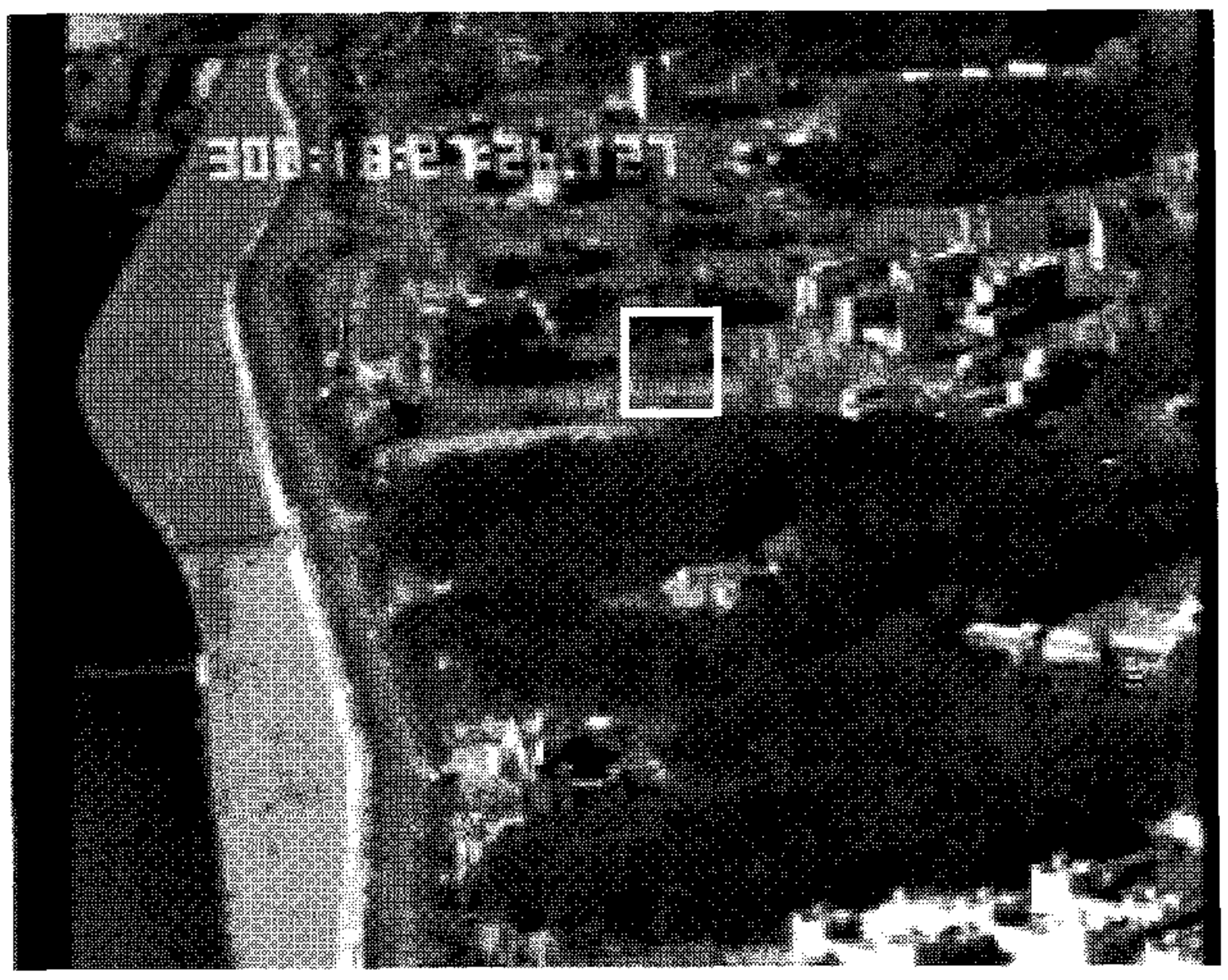

Fig. 8. Reference image.

As the frame goes on, the size and shape of the target in the input image differ from those in the reference image. Therefore, the template must be updated to maintain the target track. There are many techniques to update the template [10,16]. In this paper, we don't use a complex method but a simple one for template updating. The template update equation is presented in (32)

$$T(X,Y) = \alpha T(X,Y) + (1-\alpha) I(X + X_p, Y + Y_p), \tag{32}$$

where α is the template update parameter. If α is equal to 1, the template remains in its initial state. But if α is equal to 0, the template is updated by using the current measurement's position as a new position of the template. Template update is processed one time per three frames.

The filter parameters used in PSNF-*m* follow.

$$\Phi = \begin{bmatrix} 1 & 0 & 1 & 0 \\ 0 & 1 & 0 & 1 \\ 0 & 0 & 1 & 0 \\ 0 & 0 & 0 & 1 \end{bmatrix}, \quad Q = \begin{bmatrix} 100 & 0 & 0 & 0 \\ 0 & 100 & 0 & 0 \\ 0 & 0 & 0.1 & 0 \\ 0 & 0 & 0 & 0.1 \end{bmatrix}, \tag{33}$$

$$P_0 = \begin{bmatrix} 100 & 0 & 0 & 0 \\ 0 & 100 & 0 & 0 \\ 0 & 0 & 0.1 & 0 \\ 0 & 0 & 0 & 0.1 \end{bmatrix}, \quad R = \begin{bmatrix} 2^2 & 0 \\ 0 & 2^2 \end{bmatrix}, \tag{34}$$

$$P_G = 0.99, \quad \lambda = 0.0016. \tag{35}$$

We assume that the maximum number of measurement *m* is 13. The mean clutter density λ is given by $\lambda = \frac{m-1}{V_G}$. Also $\bar{P}_A(m)$ related to the number of m is needed for the filter update step and track score calculation. Because it varies with the distribution of the clutter and target amplitude, it is given from the table made in advance in case of the σ, standard deviation of Gaussian noise being equal to 15, and the m varying from 1 to 13.

When the σ of the Gaussian noise added to the input image is equal to 15, the detecting probability P_D is gained from the distribution of the clutter and target amplitude. According to the distribution of the clutter and target amplitude assumed such as Fig. 3, P_D=0.815.

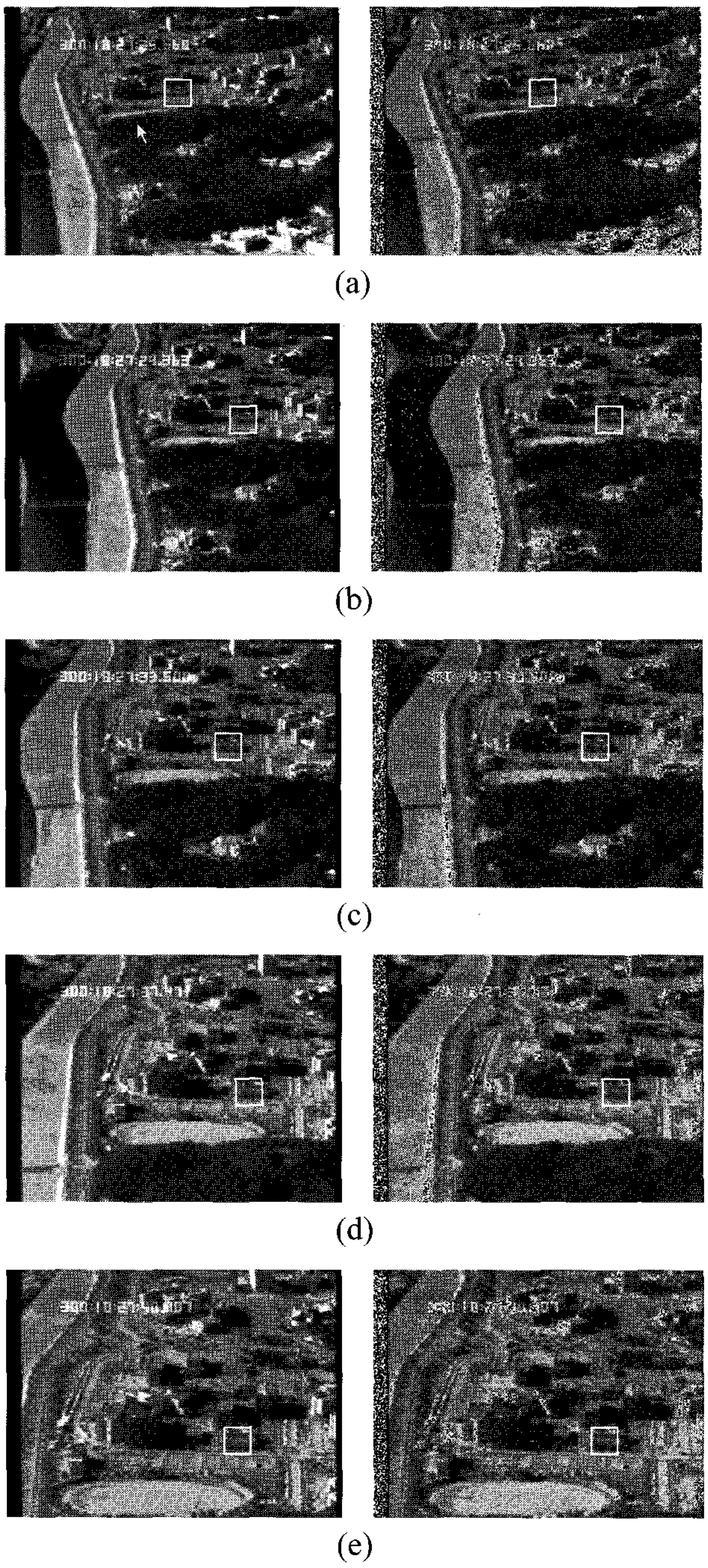

Fig. 9. (a) Beginning frame (b) Frame #100 (c) Frame #200 (d) Frame #300 (e) Final Frame.

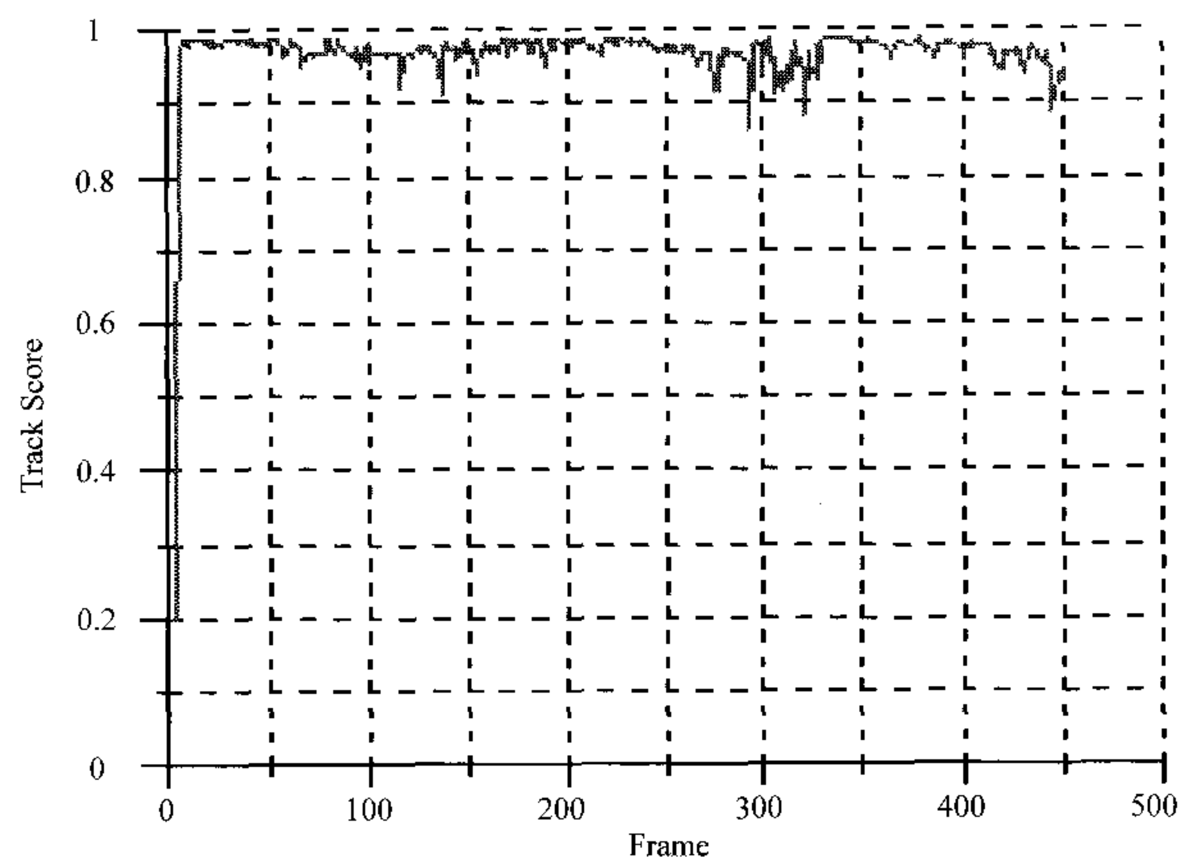

Fig. 10. The change of the track score value.

The threshold of the track score μ_c is resolved by P_D and it is set on 0.75 when the σ=15. If μ_k does not exceed μ_c in the 6th frame, the track isn't initiated.

From Fig. 9(a) to Fig. 9(e), the pictures show the simulation results on the condition of σ=15 for each frame respectively.

The left images are original input images and the rights are noise-added. Though the position and the size of target vary continuously, the tracking filter traces the target constantly. Fig. 10 shows the plot of track score.

We must examine the accuracy of filter estimates to analyze filter performance. The filter state error between the true target state and the filter estimate state has to be examined to do that; it is impossible, however, to know the true target state for each frame because of the characteristics of the image target. Therefore, we assume that the SN measurement in the VG is the true target and its position is the true one. The filter state error is calculated from the SN measurement and filter estimates. The PSNF-*m* performance is evaluated by comparing the SN measurement with the filter estimate.

Fig. 11 shows the estimation error histories of X and Y axes versus image frame numbers. They represent deviations between the true target position and the estimated position in X and Y coordinates. The results indicate that the proposed filter structure has a good target tracking performance as the errors are bounded within 2 pixels throughout the entire engagement.

Next, we carry out the simulation without template updating to check whether the track score can be used as the index of track initiation and maintenance or not. Without template updating, target loss occurs some frames later because the template still remains the

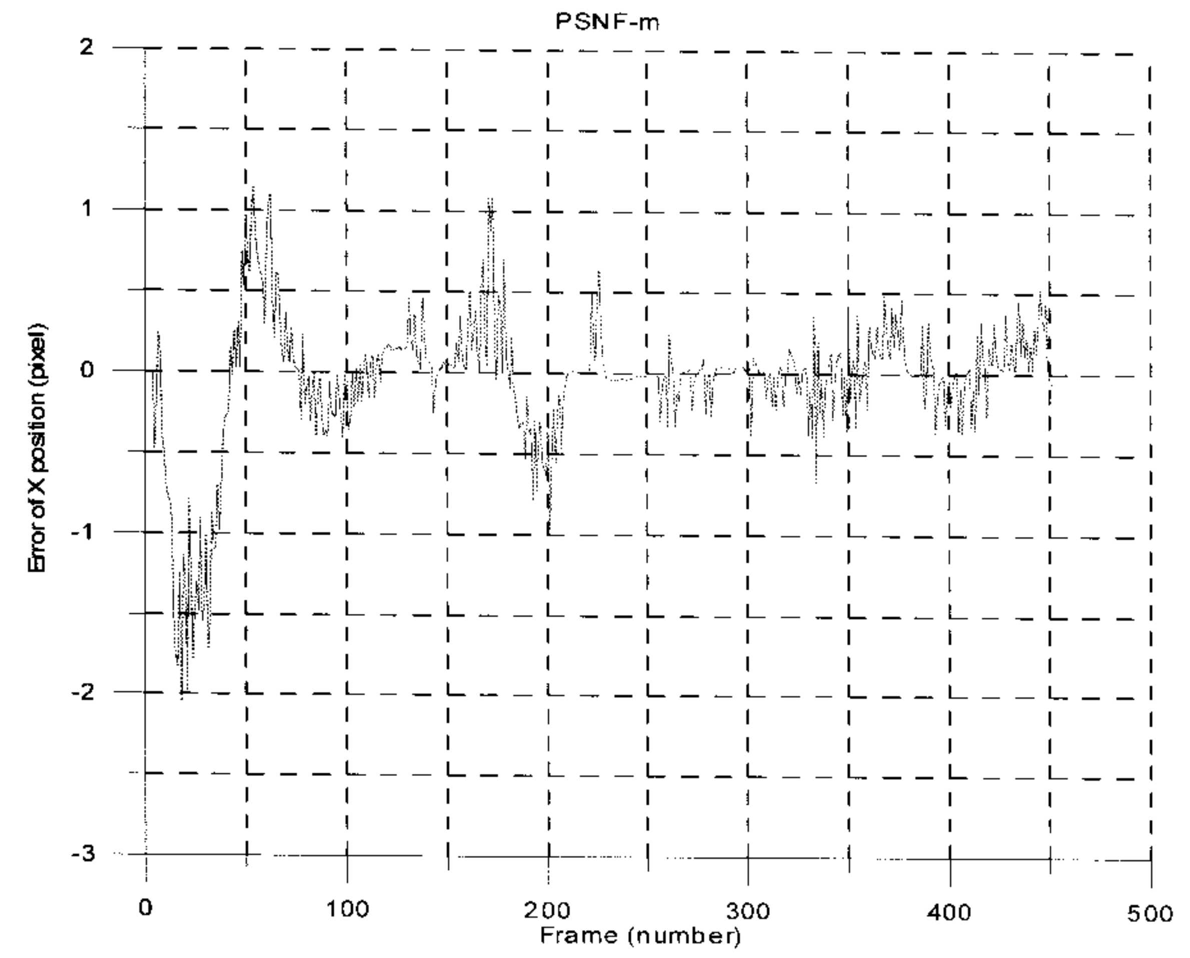

(a) *X*-axis

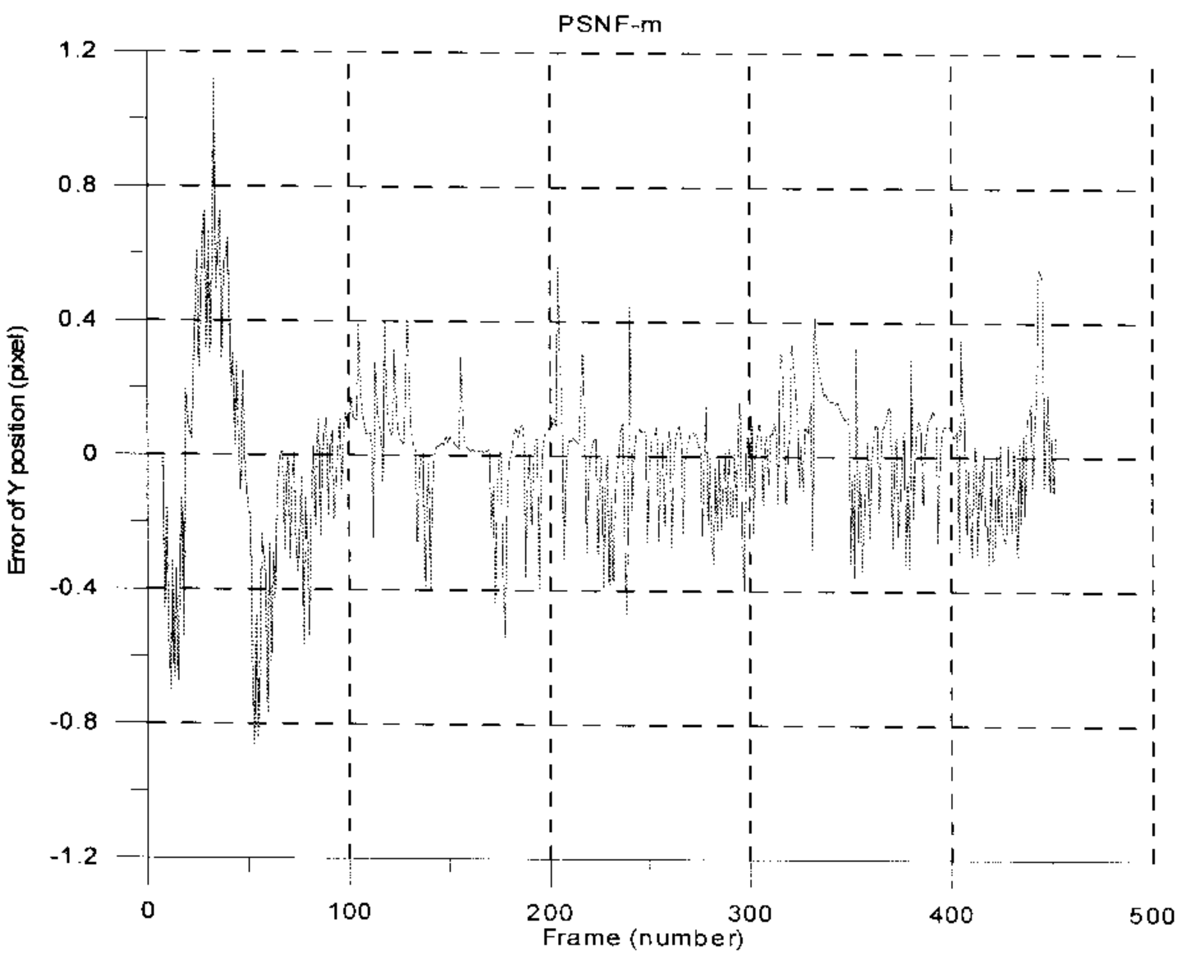

(b) *Y*-axis

Fig. 11. Estimate error histories.

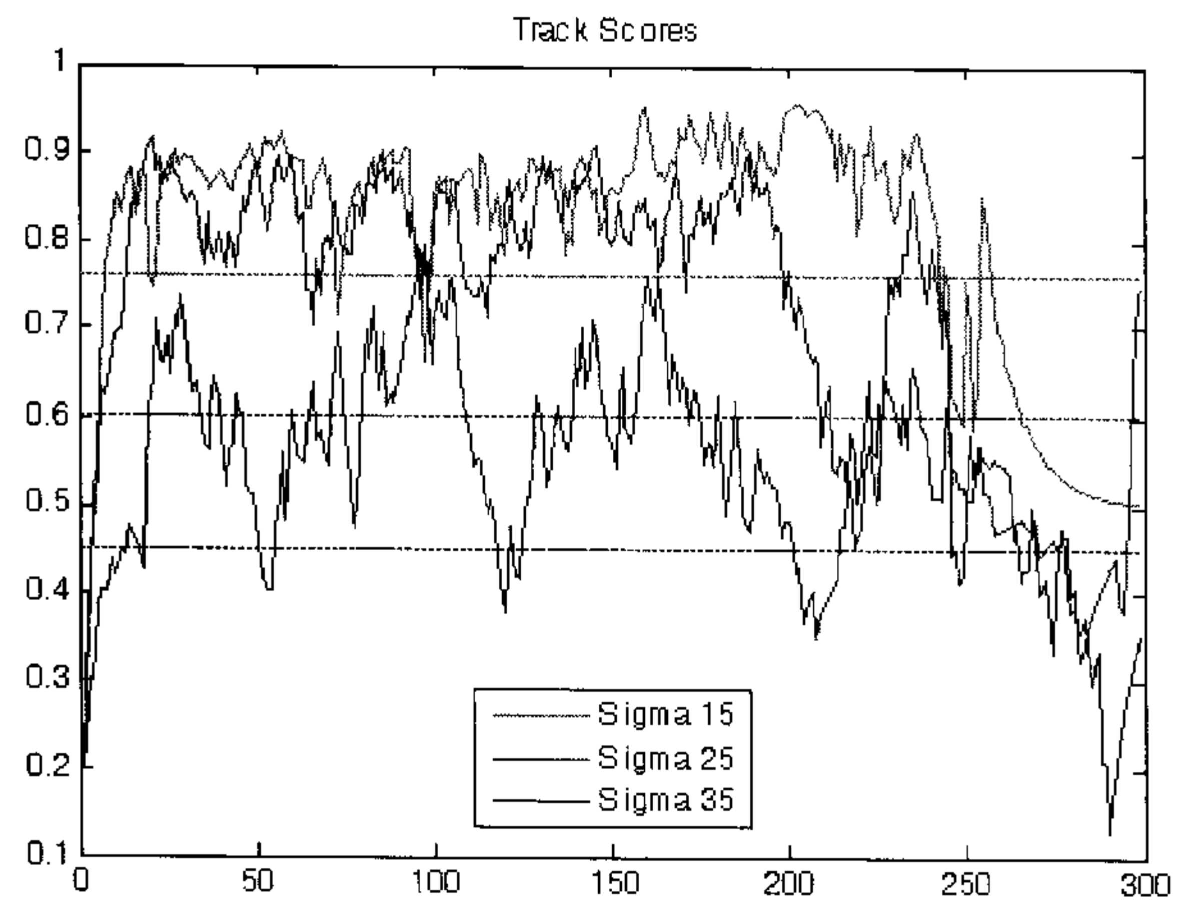

Fig. 12. The change of track score without template update.

initial one notwithstanding the target shape and size change. Fig. 12 represents the comparison result of the track score change when the template is not updated in various noisy environments.

Table 2. Comparison of run time of simulation.

	σ=15		σ=25	
	*TM-PSNFm	**Only TM	TM-PSNFm	Only TM
Run Time	21 sec	51 sec	33 sec	125 sec

* TM-PSNFm : Proposed template matching algorithm combined with PSNF-m
**Only TM : Template matching algorithm in which dynamic filter is not included.

Target loss occurs near 200 frames later in every noisy environment, and the track score decreases. If the track score μ_k is less than the μ_c, the track is regarded as having lost the target. Consequently, it is possible to decide whether to maintain the track or not by using the track score.

We will compare the proposed algorithm with a conventional template matching algorithm in which the dynamic filter is not included.

In tracking by using the template matching algorithm with which the dynamic filter is not combined, it is a problem that the calculation time is increased since matching is being carried out to the whole area of the input image. Therefore, the pyramid structure template matching method is widely used to reduce the time of matching [9].

Table 2 shows the comparison of run time of the proposed algorithm and the template matching algorithm in which the dynamic filter is not included. Two types of Gaussian noise whose σ=15 and 25 are added to the input image. The movie used in simulation has a total of 298 frames and its frame rate is 30 frames/sec.

As one can see from Table 2, the template matching algorithm without employing a dynamic filter structure takes more simulation time than the proposed algorithm. This is due to the fact that if the template matching algorithm, unlike the proposed algorithm, once fails in isolating the target, it tries to find the target with a predetermined search pattern inside an enlarged validation gate as a part of realizing the pyramid structure.

Figs. 13 and 14 represent comparison of tracking results at the final frame in case of σ=15 and σ=25. (a) is the result of the algorithm proposed in this paper and (b) is the result of the template matching algorithm in which dynamic filter is not included.

The white boxes depicted in Fig. 13 and 14 indicate the estimated target positions. The size of the box is the same as the size of the template and its center represents the target position. The results of Fig. 13 and 14 show that the proposed algorithm has a better tracking performance than a conventional template matching algorithm which does not employ a dynamic filter structure.

(a) TM-PSNFm. (b) Only TM.

Fig. 13. Target tracking result in case of σ=15.

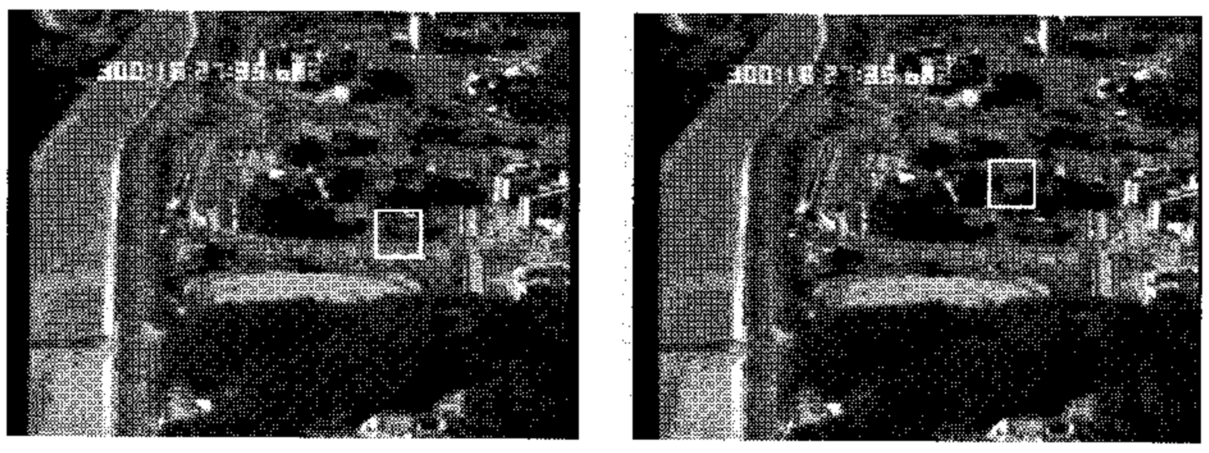

(a) TM-PSNFm. (b) Only TM.

Fig. 14. Target tracking result in case of σ=25.

5. CONCLUSIONS

A new image target tracking algorithm, combining template matching with data association and dynamic filter called PSNF-*m*, is proposed and simulation results are presented in this paper.

The measurements of the filter are formed by the template matching method widely used in image tracking, and we show that the numbers of measurements can be regulated by the GOCA-CFAR algorithm. Also, we show that the target can be tracked robustly by applying the PSNF-*m* algorithm, which is the improved form of PSNF, in an environment to which Gaussian noise is added, and we show that the track score is available in initiating the filter track and deciding whether to maintain the track or not.

The result of comparing the proposed algorithm with the template matching algorithm without dynamic filter is also represented.

REFERENCES

[1] Y. Bar-Shalom and E. Tse, "Tracking in a cluttered environment with probabilistic data association," *Automatica*, vol. 11, pp. 451-460, 1975.

[2] T. L. Song, K. J. Rhee, and D. G. Lee, "A probabilistic strongest neighbor filter algorithm for m validated measurements," *Proc. of the 7th International Conference on Information Fusion*, Stockholm, Sweden, pp. 1052-1058, June 28 - July 1, 2004.

[3] X. R. Li and X. Zhi, "PSNF: A refined strongest neighbor filter for tracking in clutter," *Proc. of the 35th CDC*, Kobe Japan, Dec. 1996.

[4] D. Lerro and Y. Bar-Shalom, "Interacting multiple model tracking with target amplitude feature," *IEEE Trans. on Aerospace and Electronic Systems*, vol. 29, no. 2, pp. 494-509, Apr. 1993.

[5] A. Papoulis and S. U. Pillai, *Probability, Random Variables and Stochastic Processes*, 4th Edition, McGraw Hill, 2002.

[6] N. Li and X. R. Li, "Target perceivability and its applications," *IEEE Trans. on Signal Processing*, vol. 49, no. 11, pp. 2588-2604, Nov. 2001.

[7] M. J. Tahk, H. C. Bang, Y. D. Kim, J. Y. Choi, J. H. Seo, T. L. Song, and J. W. Choi, *Automatic Control Research Center Guidance and Control Lab.*, 3rd Step Interim Report, Agency for Defense Development, 2002.

[8] H. Chang, J. Zhang, "New metrics for clutter affecting human target acquisition," *IEEE Trans. on Aerospace and Electronic Systems*, vol. 42, no. 1, pp. 361-368, Jan. 2006.

[9] D. J. Gang and J. E. Ha, *Digital Image Processing with Visual C++*, SciTech Media, 2003.

[10] B. Lucas and T. Kanade, "An iterative image registration technique with an application to stereo vision," *Proc. of Int'l Joint Conf. Artificial Intelligence*, pp. 674-679, 1981.

[11] S. Baker and I. Matthews, "Lucas-Kanade 20 years on: A unifying framework," *International Journal of Computer Vision*, vol. 53, no. 3, pp. 221-255, 2004.

[12] R. Nitzberg, "Composite CFAR techniques," *Proc. of the 27th Asilomar Conference*, vol. 2, pp. 1133-1137, Nov. 1993.

[13] P. P. Gandhi and S. A. Kassam, "Analysis of CFAR processors in homogeneous background," *IEEE Trans. on Aerospace and Electronic Systems*, vol. 24, no. 4, pp. 427-445, Jul. 1988.

[14] S. Watts, "The performance of cell-averaging CFAR systems in sea clutter," *Proc. of Radar Conference*, pp. 398-403, May 2000.

[15] M. Barkat and F. Soltani, "Cell-averaging CFAR detection in compound clutter with spatially correlated texture and speckle," *IEE Proceedings, Radar, Sonar and Navigation*, vol. 146, no. 6, pp. 279-284, Dec. 1999.

[16] T. Kaneko and O. Hori, "Template update criterion for template matching of image sequences," *Proc. of the 16th International Conference on Pattern Recognition*, vol. 2, pp. 1-5, Aug. 2002.

[17] V. G. Hansen and J. H. Sawyers, "Detectability loss due to greatest of selection in a cell-averaging CFAR," *Proc. of the IEEE International Radar Conference*, pp. 325-332, 1973.

[18] J. D. Moore and N. B. Lawrence, "Comparison

of two CFAR methods used with square law detection of Swerling I targets," *Proc. of the IEEE international Radar Conference*, pp. 403-409, 1980.
[19] G. V. Trunk, "Range resolution of targets using automatic detectors," *IEEE Trans. on Aerospace and Electronic Systems*, vol. 14, pp. 750-755, Sep. 1978.
[20] H. Rohling, "Radar CFAR thresholding in clutter and multiple target situations," *IEEE Trans. on Aerospace and Electronic Systems*, vol. 19, pp. 608-621, Jul. 1983.
[21] H. Rohling, "New CFAR processor based on ordered statistic," *Proc. of the IEEE International Radar Conference*, pp. 38-42, 1984.
[22] J. T. Rickard and G. M. Dillard, "Adaptive detection algorithm for multiple target situations," *IEEE Trans. on Aerospace and Electronic Systems*, vol. 13, pp. 338-343, Jul. 1977.
[23] G. V. Trunk, B. V. Cantrell, and F. D. Queen, "Modified generalized sign test processor for 2-D radar," *IEEE Trans. on Aerospace and Electronic Systems*, vol. 10, pp. 574-582, Sep. 1974.
[24] J. A. Ritcey, "Censored mean-level detector analysis," *IEEE Trans. on Aerospace and Electronic Systems*, vol. 22, pp. 443-454, Jul. 1986.

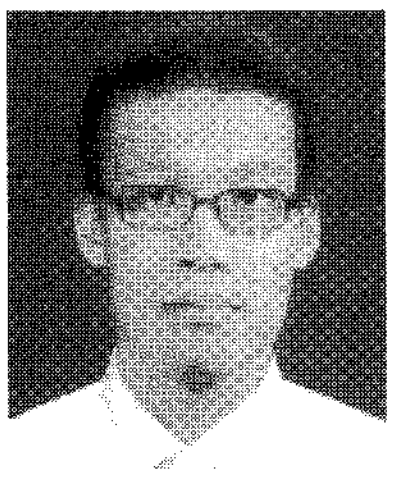

Jong-Sue Bae received the M.S. degree in Electronics, Electrical, Control and Instrumentation Engineering from Hanyang University in 2002. His research interests include target tracking systems, image processing, guidance and control.

Taek-Lyul Song received the Ph.D. degree in Aerospace Engineering from University of Texas at Austin in 1983. His research interests include target state estimation, guidance, navigation and control.